APPLIED ECOLOGY

Biocrusts protect the Great Wall of China from erosion

Yousong Cao[1,2,3], Matthew A. Bowker[4,5], Manuel Delgado-Baquerizo[6], Bo Xiao[1,2,3,7]*

The Great Wall of China, one of the most emblematic and historical structures built by humankind throughout all of history, is suffering from rain and wind erosion and is largely colonized by biocrusts. However, how biocrusts influence the conservation and longevity of this structure is virtually unknown. Here, we conducted an extensive biocrust survey across the Great Wall and found that biocrusts cover 67% of the studied sections. Biocrusts enhance the mechanical stability and reduce the erodibility of the Great Wall. Compared with bare rammed earth, the biocrust-covered sections exhibited reduced porosity, water-holding capacity, erodibility, and salinity by 2 to 48%, while increasing compressive strength, penetration resistance, shear strength, and aggregate stability by 37 to 321%. We further found that the protective function of biocrusts mainly depended on biocrust features, climatic conditions, and structure types. Our work highlights the fundamental importance of biocrusts as a nature-based intervention to the conservation of the Great Wall, protecting this monumental heritage from erosion.

INTRODUCTION

The Great Wall of China stretches an astonishing 8851.8 km across mostly dryland environments and is recognized as a world heritage site due to its unparalleled construction duration and geographical span (*1*). Enduring for over five centuries, the Great Wall serves as an irreplaceable manifestation of the Chinese nation and an invaluable treasure of human civilization. The Great Wall in many locations and time periods was built with rammed earth, which was one of the most common materials used to build large structures in the ancient world, encompassing natural raw materials such as soil and gravel and was used to build walls and foundations (*2*). Currently, these types of structures (i.e., earthen heritage sites) constitute approximately 10% of the World Heritage List, most of which are found in dry climate regions of Central Eurasia. As an emblematic rammed earth structure (*3*, *4*), the Great Wall is highly vulnerable to wind erosion, rainfall scouring, salinization, and freeze-thaw cycles, leading to severe issues such as cracking, disintegration, and even eventual collapse (*5*, *6*). Considering the impacts of global climate change, the Great Wall is at risk of severe deterioration, which may jeopardize the long-term durability of its rammed earth structure (*7*). As of now, only 5.8% of its total length remains well preserved, while 52.4% has either vanished or become severely deteriorated (*8*). Therefore, conservation strategies must be implemented as a matter of urgency. Implementing more effective and sustainable strategies to mitigate the deterioration is critical for conserving this invaluable cultural heritage for future generations (*9*, *10*).

Traditional heritage conservation theory suggests that natural vegetation is harmful and must be removed from the heritage structure due to the destruction from root activity and biological weathering (*11*), but studies conducted over the past three decades challenge this viewpoint, revealing that short-rooted and drought-resistant herbs can serve as a natural protector against erosion rather than a destroyer (*12*, *13*). Nonetheless, the influence of vegetation on the conservation of large-scale human-made structures is still under debate. Biocrusts, photoautotrophic communities primarily composed of cyanobacteria, mosses, lichens, other microorganisms, and tightly bound soil particles (*14*–*16*), are known to cover large sections of the Great Wall (*17*). Although biocrusts colonize only a few centimeters on the surface soil, they can act as ecosystem engineers supporting and regulating many key processes of soil and terrestrial ecosystems (*18*), including hydrology (*19*), substrate stability (*20*), biogeochemical cycles (*21*), and vegetation succession (*22*). Hence, biocrusts may also influence the mechanical stability and physicochemical properties of the rammed earth used to build the Great Wall, serving as a natural living cover to protect earthen heritage objects in dry climates (*23*). However, the contribution of biocrusts to conserving the Great Wall is virtually unknown.

Here, we hypothesized that similar to their effect on natural soils, biocrusts can increase the stability, as well as reduce the erosion, of the Great Wall. To test this hypothesis, we conducted an extensive biocrust survey on the Great Wall to investigate the influence of biocrusts on the stability and erodibility of the Great Wall. Our survey expands over 600 km in the drier climate section of the Great Wall. Our sampling was conducted on the rammed earth material of the Great Wall and targeted bare surfaces (uncovered by vegetation or biocrusts; bare rammed earth hereafter) and biocrust-covered sections of the Great Wall. Subsequently, laboratory analyses of the biocrusts (cyanobacteria and moss-dominated) and bare rammed earth were carried out. Our study proves that the colonization and development of biocrusts exert long-term and multifaceted protections against erosion on the Great Wall through enhancing mechanical stability and reducing the erodibility of rammed earth. This knowledge provides a momentous insight and nature-based intervention for global heritage conservation in drylands.

[1]The Research Center of Soil and Water Conservation and Ecological Environment, Chinese Academy of Sciences and Ministry of Education, Yangling, China. [2]State Key Laboratory of Soil Erosion and Dryland Farming on the Loess Plateau, Institute of Soil and Water Conservation, Chinese Academy of Sciences and Ministry of Water Resources, Yangling, China. [3]University of Chinese Academy of Sciences, Beijing, China. [4]School of Forestry, Northern Arizona University, Flagstaff, AZ, USA. [5]Center of Ecosystem Science and Society, Northern Arizona University, Flagstaff, AZ, USA. [6]Laboratorio de Biodiversidad y Funcionamiento Ecosistémico, Instituto de Recursos Naturales y Agrobiología de Sevilla (IRNAS), CSIC, Seville, Spain. [7]Key Laboratory of Arable Land Conservation (North China), Ministry of Agriculture and Rural Affairs/College of Land Science and Technology, China Agricultural University, Beijing, China.
*Corresponding author. Email: xiaobo@cau.edu.cn

RESULTS

Biocrusts cover large sections of the Great Wall

We found that cyanobacteria and moss biocrusts covered 67.1% of the studied sections of the Great Wall. Thus, the Great Wall seems to provide a favorable environment for cyanobacterial and moss biocrusts. Biocrust-forming lichens were also found occasionally (fig. S1). These biocrusts were composed of different dominant species (table S5). In general, *Tychonema* was the dominant genus in the cyanobacterial biocrusts, and *Leptolyngbya*, *Microcoleus*, *Chroococcidiopsis*, *Mastigocladopsis*, and *Diplosphaera* were common additional genera. The moss-dominated biocrusts, on the other hand, were dominated by the family *Pottiaceae*, encompassing *Didymodon* Hedw. and *Barbula* Hedw. (fig. S2). Furthermore, we also found two types of lichen biocrusts on the Great Wall, *Cladonia phyllophora* Ehrh. ex Hoffm. and *Ochrolechia* sp.

We found that the characteristics of biocrusts covering the Great Wall varied with the biocrust type, climate, and type of structure (e.g., wall and fortress of the Great Wall) (see table S3). For instance, cyanobacterial biocrusts were the dominant types of biocrusts covering the Great Wall in arid climates, covering 1.5 times more surface than in semiarid climates. Contrastingly, moss biocrusts thrive in wetter semiarid climates, supporting a 44.1% more moss cover than in arid climates. Furthermore, the development level of biocrusts was especially noticeable in the fortresses. Biocrusts supported 11.9 to 88.0% more cover and greater thickness and biomass on the fortresses compared with the walls. As shown in table S4, the factors of biocrust type, climate, and structure type all had significant effects on biocrust characteristics, with their interaction effects being also statistically significant.

Biocrusts protect the Great Wall from erosion

Our analyses revealed that biocrusts play a critical role in reducing the levels of natural erosion of the Great Wall. Biocrusts were found to reduce the capillary and total porosity of rammed earth (bare rammed earth > cyanobacterial biocrusts > moss biocrusts) and cause a reduction of field capacity by 5.2% on average (Fig. 1C). Specifically, field capacity is a critical soil hydraulic parameter defined as the soil water content when the capillary-suspended water reaches its maximum, reflecting soil water retention property and influencing runoff, evaporation, and infiltration. Thus, the lower field capacity of biocrusts indicated their potential to reduce infiltration into the wall. Meanwhile, the porosity of biocrusts in arid climates was 1.1 times greater than in semiarid climates (Fig. 1, A and B), suggesting a potential impact of climate conditions on biocrust properties. Moreover, variations were also observed in the porosity and water-holding capacity of biocrusts across different structure types of the Great Wall, and there were also differences among various defense districts (i.e., the military-political division of the Great Wall in the Chinese Ming Dynasty) on the regional scale (Fig. 1, A, B, and D, and fig. S4). Moss biocrusts on the fortresses demonstrated a 5.5 to 22.6% decrease in porosity and water-holding capacity compared with that on the walls, indicating that the contribution of moss biocrusts to strengthening the infiltration resistance is especially important for fortresses (Fig. 1, A and B). Among four defense districts, the defense district with the lowest porosity and water-holding capacity of biocrusts was 2.2 to 11.2% lower than other defense districts, reflecting the different biocrust effects caused by its diverse development status in distinct microclimates of each district.

Biocrusts promoted the mechanical stability of the Great Wall against external erosive forces (Fig. 2 and fig. S5). Notably, under external pressure, the stress-strain curves of biocrusts and bare rammed earth had different peak values, representing contrasting compressive strength (Fig. 2A). Biocrusts had 124% (168.59 kPa versus 75.07 kPa), 37% (0.97 MPa versus 0.71 MPa), and 53% (5.61 kg/cm^2 versus 3.66 kg/cm^2) higher compressive strength, penetration resistance, and shear strength, respectively, than bare rammed earth (Fig. 2, B to D). In addition, the mechanical stability of moss biocrusts surpassed that of cyanobacterial biocrusts. Regarding the climatic influence (Fig. 2D and fig. S5, D and E), the penetration resistance of biocrusts in arid climates was 1.4 times that in semiarid climates, while the compressive strength and shear strength were lower than those in semiarid climates. Furthermore, the mechanical stability of biocrusts varied with structure types of the Great Wall (Fig. 2E and fig. S5F). Specifically, the compressive strength of biocrusts on fortresses was 1.6 times that on the walls, while the shear strength was 12.4% lower than that on walls; in contrast, there was little difference in compressive strength of bare samples from walls and fortress.

Biocrusts were found to significantly reduce the erodibility of the Great Wall, which was evidenced by the 178% increase in aggregate stability (Fig. 3, A to C), 142% increase in organic matter content (fig. S7A), 40% decrease in soluble salt content (Fig. 3D), and 48% decrease in electrical conductivity (Fig. 3E). The erodibility (***K***), which reflects the vulnerability of soil to erosion, is positively correlated with the rate of soil loss. We found that moss biocrusts in semiarid climates reduced erodibility (***K***) by 14.8% (0.148 versus 0.194), further indicating the positive influence of biocrusts on the Great Wall (Fig. 3F). Furthermore, the macroaggregate content, geometric mean diameter (GMD), and mean weight diameter (MWD) of biocrusts on fortresses were similar to that on the walls, but these indicators of fortress exhibited higher values than walls if there was no biocrust cover (fig. S6, A to C). On the regional scale, the above differences were ultimately reflected as the variations of erodibility in different defense districts of the Great Wall (Fig. 3G and figs. S6, D to F, and S7, D and E). The defense district with the greatest aggregate stability was 11.2 to 62.5% higher than others, while the defense district with the lowest erodibility and salinity was 4.5 to 38.5% lower than others.

Relationship between biocrust characteristics and their protective functions

As illustrated in fig. S8, we found that the protective functions of biocrusts were closely correlated with their fundamental physicochemical characteristics. With regard to cyanobacterial biocrusts, their porosity had negative correlations with compressive strength ($r = -0.73$), aggregate stability ($r = -0.90$), and organic matter content ($r = -0.90$). Simultaneously, the thickness of biocrust layer demonstrated a negative correlation with electrical conductivity ($r = -0.76$), while organic matter content manifested positive correlations with aggregate stability ($r = 0.96$). For moss biocrusts, we found positive correlations between moss density and aggregate stability ($r = 0.90$). In addition, organic matter content had positive relationships with aggregate stability ($r = 0.88$) and erodibility ($r = 0.71$), while it had a negative correlation with field capacity ($r = -0.74$).

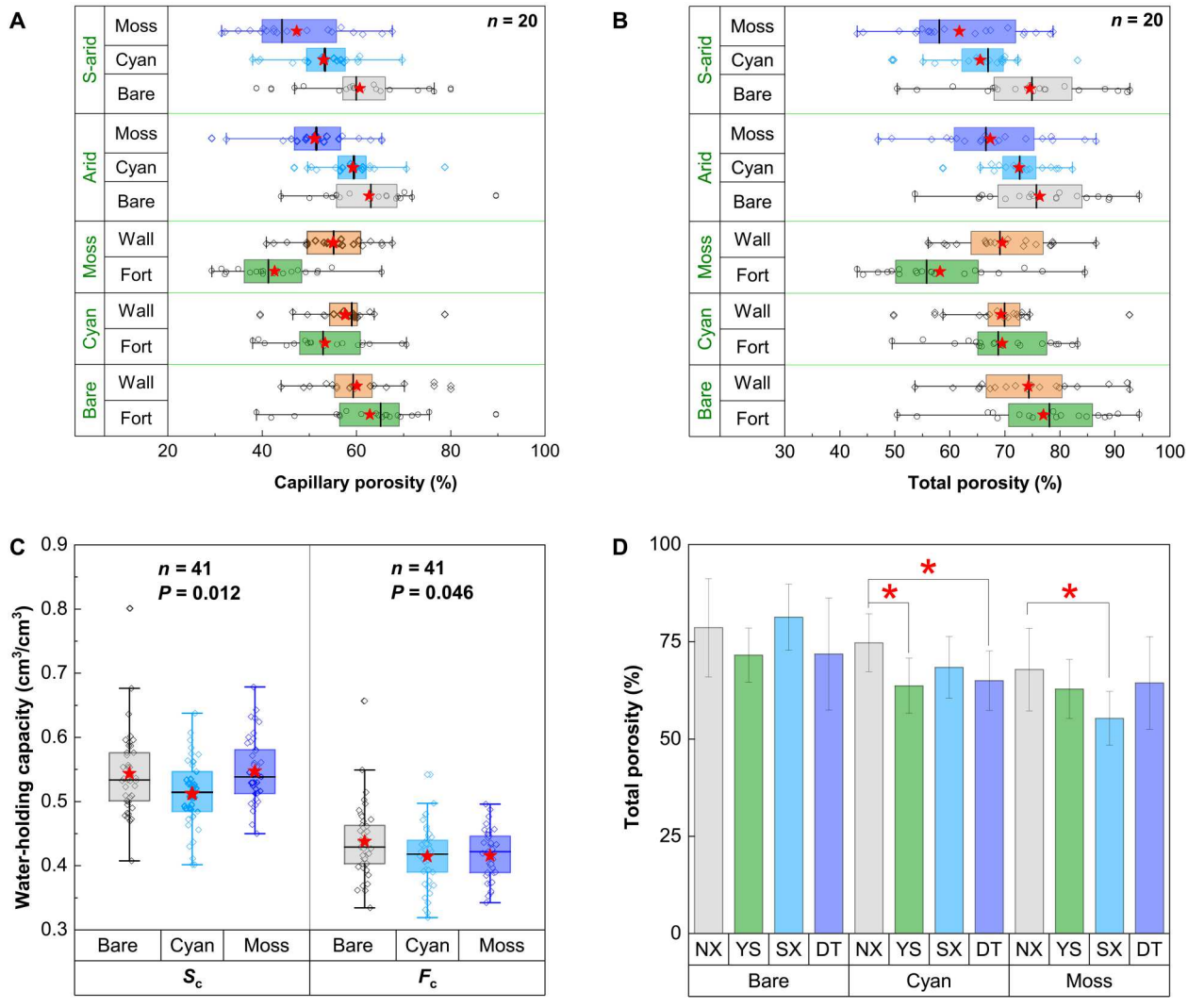

Fig. 1. Porosity and water-holding capacity of biocrusts and bare rammed earth on the Great Wall. (**A**) Box chart of capillary porosity of bare (bare rammed earth), cyan (cyanobacterial biocrusts), and moss (moss biocrusts) in different climates (arid, arid climate; S-arid, semiarid climate) and structure types (wall; fort, fortress). The red stars indicate the mean value. (**B**) Box chart of total porosity. (**C**) Box chart of S_c (saturated water content) and F_c (field capacity). (**D**) Total porosity in different defense districts (NX, Ningxia; YS, Yansui; SX, Shanxi; DT, Datong). The * designates a significant difference between different defense districts at the 0.05 level of probability.

DISCUSSION

Our study highlights the contribution of biocrusts to protect a large section of the Great Wall from natural erosion. Biocrusts were dominant organisms covering this irreplaceable and unparalleled monument of human heritage and provided greater stability and lower erodibility compared with bare sections. This knowledge is critical to understand how living covers influence the long-term conservation of one of the most important human monuments ever made.

Biocrusts currently cover a large portion of the Great Wall

We found that biocrusts were dominant organisms covering the Great Wall. More than two-thirds of the studied sections were covered by biocrusts, encompassing filamentous cyanobacteria (e.g., *Tychonema* and *Leptolyngbya*), globular cyanobacteria (e.g., *Chroococcidiopsis* and *Diplosphaera*), and *Pottiaceae* family mosses. According to the morphological classification and definition of the biocrust type (*24*–*26*), the biocrusts should be classified as pinnacled crusts, which occur in mid-latitude cool deserts with arid and semiarid climates and are dominated by cyanobacteria. Regarding morphology, these biocrusts were characterized by pinnacled mounds with mosses colonizing on their tips during the succession, which can eventually support over 40% moss cover.

The formation and functions of biocrusts were mainly derived from the above dominant organisms (*27*), which exhibit remarkable cohesion effects, promoting the formation of a biocrust layer through enmeshment of soil particles in stringy biological structures (e.g., moss rhizoids and cyanobacterial filaments) and through secretion of soil binding compounds such as extracellular polymeric substances (EPSs; including polysaccharides, amino acids, proteins, etc.) (*28*, *29*). As pioneer species with exceptional stress resistance, cyanobacteria have evolved a robust cell wall and often protect themselves in gelatinous masses of EPS against desiccation and radiation, and they have the ability to isolate themselves from detrimental microhabitats through phototaxis (*30*, *31*),

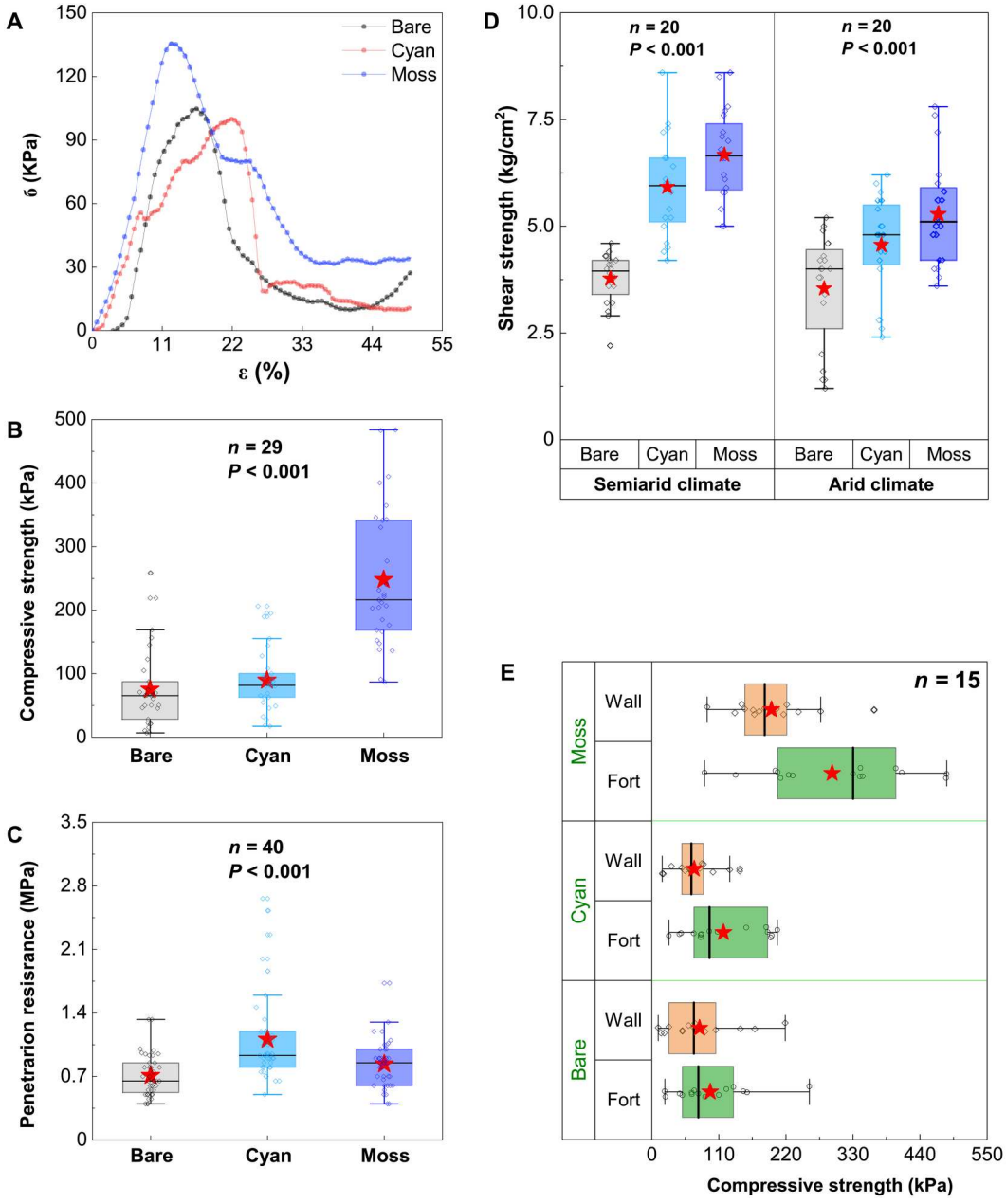

Fig. 2. Mechanical stability of biocrusts and bare rammed earth on the Great Wall. (**A**) ε (strain) and **δ** (stress) curve of bare (bare rammed earth), cyan (cyanobacterial biocrusts), and moss (moss biocrusts). (**B**) Box chart of compressive strength. The red stars indicate the mean value. (**C**) Box chart of penetration resistance. (**D**) Box chart of shear strength in different climate regions. (**E**) Box chart of compressive strength in different structure types (wall; fort, fortress).

making them well suited to growth on the surface of the Great Wall. Similarly, some mosses have developed specialized drought-tolerance structures, such as C-shaped or circular cell papillae (*32*), which have the mechanisms of reflecting radiation and promoting water conduction (*33*), thus enabling them to adapt to environmental stress on the Great Wall featuring high temperatures, drought, and intense solar radiation. Therefore, the stable colonization and long-term development of biocrusts on the Great Wall can be essentially attributed to the stress resistance of cyanobacteria and mosses within it.

Biocrusts protect the Great Wall from further erosion

We found that biocrusts play an essential role in reducing erosion in the Great Wall compared with bare walls. As shown in Fig. 4, biocrusts exert protective functions in the Great Wall through multifaceted pathways. First, the dense biomass at the surface of biocrusts serves as an anti-infiltration layer (*34*), resulting in the blockage of soil pores connecting the surface to the deeper substrate and therefore reducing porosity and water-holding capacity (*35*), which helps to maintain a dry environment inside the heritage structure and prevent disintegration and hydrolysis caused by

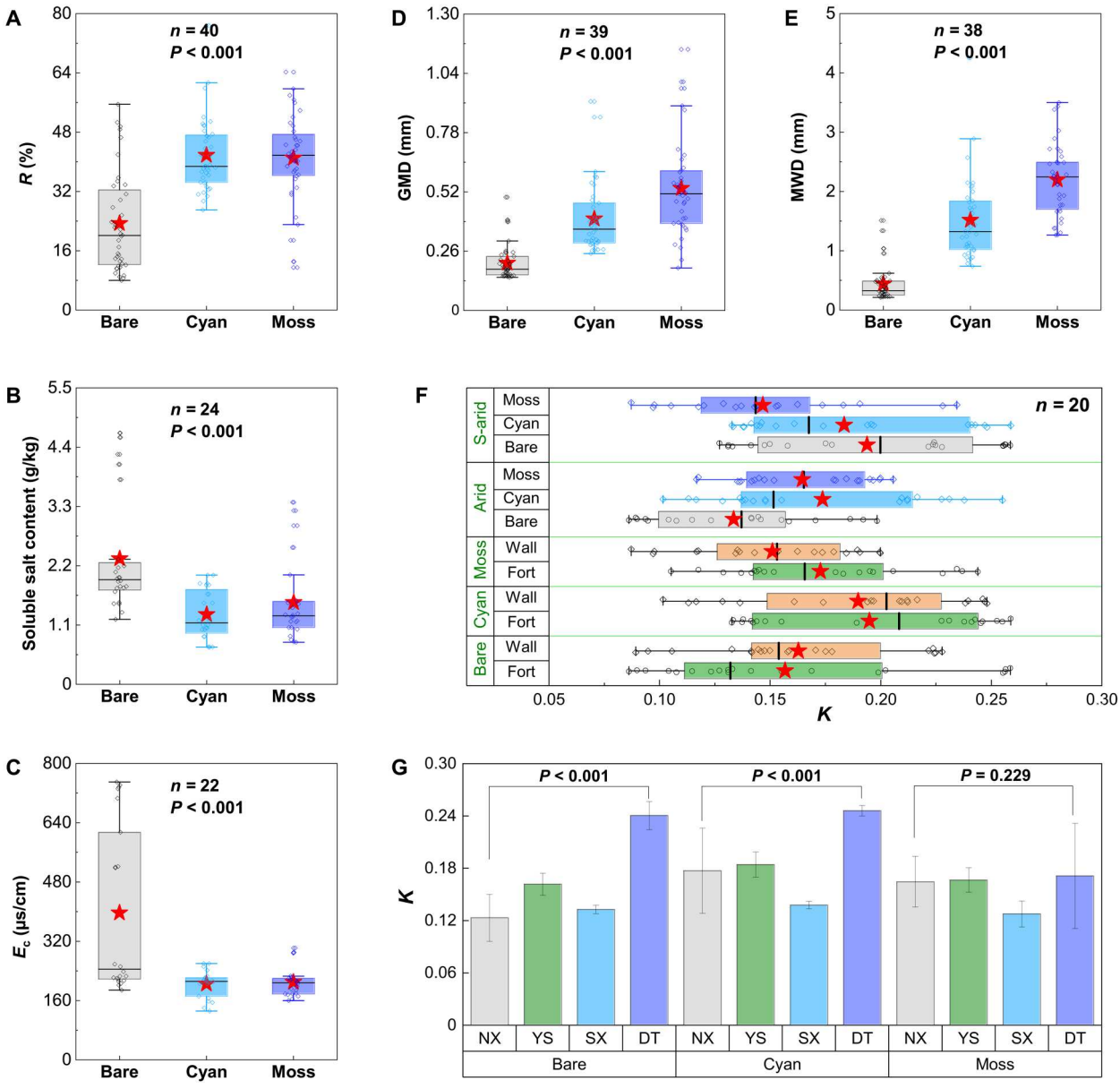

Fig. 3. Erodibility indicators of biocrusts and bare rammed earth on the Great Wall. (**A**) Box chart of ***R*** (macroaggregate content) of bare (bare rammed earth), Cyan (cyanobacterial biocrusts), and Moss (moss biocrusts). The red stars indicate the mean value. (**B**) Box chart of soluble salt content. (**C**) Box chart of E_c (electrical conductivity). (**D**) Box chart of GMD. (**E**) Box chart of MWD. (**F**) Box chart of ***K*** (erodibility coefficient) in different climates (arid climate and semiarid climate) and structure types (wall and fortress). (**G**) ***K*** in different defense districts (Ningxia, Yansui, Shanxi, and Datong).

frequent wet-dry cycles (*36*). In addition, the soil-binding secretions and filamentous structures of biocrusts interweave to form a sticky network that wraps soil mineral particles and aggregates (*37*), promoting mechanical strength and aggregate stability against external erosive forces (*38*, *39*). Moreover, biocrusts continually absorb soluble base cations from the substrate to synthesize metabolic compounds, resulting in the mitigation of heritage salt corrosion (*40*, *41*). Furthermore, the carbon fixation of biocrusts enhances soil organic matter content, indirectly promoting aggregate stability and reducing the erodibility of rammed earth (*42*). Meanwhile, biocrusts function as a thermic blanket, buffering against soil temperature fluctuations and preventing heritage structures from swelling-shrinkage deformation and freeze-thaw damage (*43*).

On the other hand, it should be pointed out that the biocrust-forming cyanobacteria, mosses, and lichens may also exert some potential biodeteriorative effects on the heritage site. Previous studies have revealed the biological corrosion and weathering of cryptogams and microorganisms on stone heritages, including the mechanical damage of roots and filaments, expansion of organisms, biomineralization, and acidic secretions (*44*–*46*). However, the biocrust effects on earthen heritages are very different from lichens on stone heritages. First, soil has a loose and porous structure that is

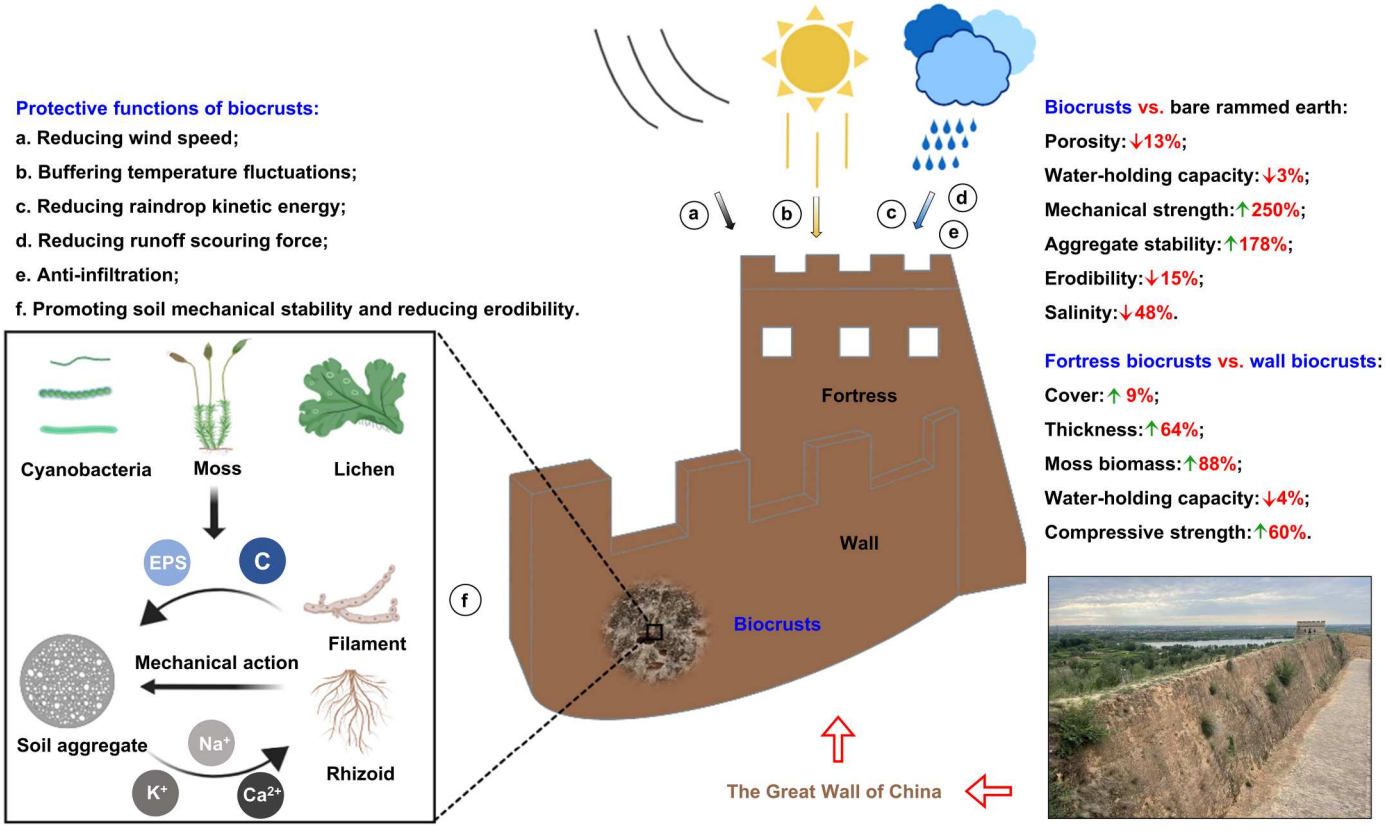

Fig. 4. Diagram showing the overall protective functions of biocrusts against erosion in the Great Wall as well as the influencing pathways. In comparison to bare rammed earth, biocrusts exert protective effects mainly by reducing erosive force, strengthening soil mechanical stability, and reducing soil erodibility. The developmental level and protective function of biocrusts on fortresses surpassed that on walls. EPS, extracellular polymeric substances. C means other organic matter such as exudate, secretion, mucilage, and sloughed residue.

different from stones, which can buffer the mechanical action from biocrust filaments. Meanwhile, given that earthen heritages are mainly distributed in arid and semiarid climate regions, the chemical corrosion and weathering that require water as the reaction medium are weak, and the intense wind and water erosion are the primary threats (*3*, *5*). Thus, the protective function of biocrusts produced by their reduction of erodibility is much greater than the potential biodeterioration caused by their biological weathering, making the former a more noteworthy and important aspect in the protection of earthen heritages. Furthermore, another potential biodeterioration could be caused by the high cover of biocrusts, which may disfigure the original appearance and aesthetics of earthen heritage sites. Some previous studies have mentioned the impact of vegetation and biofilms on the aesthetic value of heritage sites (*47*, *48*), but the maximum acceptable cover of vegetation without affecting the original aesthetics remains uncertain. As a relatively subjective issue, aesthetics is difficult to develop a unified standard. In addition, the acceptance of vegetation cover may vary among heritages in different environments and styles. Therefore, as an important and interesting topic, the biocrust effect on the aesthetics of heritage sites deserves further study and discussion.

The contribution of biocrusts to the conservation of the Great Wall is context dependent

The protective functions of biocrusts were closely correlated with their types and developmental levels and therefore varied with climate regions, structure types, and defense districts of the Great Wall. Specifically, cyanobacterial and moss biocrusts had distinct habitat preferences; the more effective protectors were mosses that were more prevalent in semiarid rather than arid climates. These two groups are also part of a common successional sequence from early successional cyanobacteria, transitioning to mosses where the climate permits (*49*). Similar climate-dominated patterns are found in biocrusts across the Negev Desert, Mojave Desert, and Colorado Plateau (*14*), and we provide further evidence to confirm that variation of biocrust type is regulated by climate (*50*). At a more advanced developmental level, moss biocrusts exceeded cyanobacterial biocrusts in thickness and biomass, with a denser surface, rhizoids stronger and thicker than cyanobacterial filaments, and more accumulation of soil organic matter (*49*, *51*). Thus, moss biocrusts exerted stronger protective functions than cyanobiocrusts under identical conditions.

Furthermore, we found that the climate conditions indirectly affected biocrust protective functions through regulating the relative abundance of moss and cyanobacterial biocrusts, which was evidenced by higher stability and lower erodibility of biocrusts in

wetter semiarid climates compared with more arid climates. Moreover, fortress and wall represent the two primary structure types of the Great Wall with different construction technologies (*52*), and the former were always constructed using fine-textured clay with less impurity considering its superior defense function, resulting in the substrate of fortresses being more conducive to the biocrust colonization and subsequently being more effectively protected by biocrusts than walls (Fig. 4). Similarly, as the composition of rammed earth and biocrust features change along the Great Wall in response to local climate and soil property variations (*53*), differences were also observed in various defense districts of the Great Wall, further reflecting the comprehensive influence of climates, microgeomorphology, and rammed earth properties on biocrust contribution to heritage conservation on the regional scale. Overall, these contrasting results underscore the necessity of considering the climate conditions and substrate characteristics of heritage structures when comprehensively evaluating the development status and protective functions of biocrusts in heritage sites as we have done here.

Biocrust provide a nature-based intervention to heritage conservation

Currently, in light of the uncertainty engendered by global climate change, the strategy for heritage conservation should be designed to address the complex interactions between heritage structures and the environment, consequently mitigating environmentally driven deterioration (*10*, *54*). Thus, the approach of heritage conservation through vegetation cover, known as "soft capping" (*13*), has been preliminarily discussed and implemented in Europe (*12*, *55*) as a nature-based, cost-effective, and long-lasting strategy and an alternative to traditional measures like "hard capping" with artificial cemented capping layer on top of heritage structure (*56*). Nevertheless, controversy persists regarding the efficacy of vegetation cover in preserving heritage structures (*45*). Against this backdrop, our study represents a comprehensive report concentrating on the positive influence of biocrusts on earthen heritage conservation, particularly through conducting an extensive investigation across arid and semiarid climates. We provided strong evidence to prove that biocrusts can help reduce erosion in the Great Wall of China supporting its conservation, which will raise the awareness of preservationists to reappraise the role of living covers on heritage structures. Although our study was focused specifically on the Great Wall, we are confident that many earthen heritage structures in drylands worldwide that are undergoing deterioration or at risk of future deterioration can also be sheltered by biocrusts. On the basis of previous studies (*15*, *57*), the cover of biocrusts colonized on the Great Wall may decrease in the face of future climate change (e.g., rising temperature and increasing precipitation) like the biocrusts in the entire dryland ecosystems, which reminds us that we cannot ignore the potential impact of climate change on the protective role of biocrusts. Fortunately, cyanobacterial biocrusts seems less adversely affected by climate change (*57*), thus making it an ideal protector under future climate change.

In summary, the utilization of biocrusts represents a promising and innovative strategy for heritage conservation as they offer superior advantages over conventional protective measures. In particular, biocrusts serve as stabilizers, consolidators, sacrificial layers, and drainage roofs, combining the protective functions of several conventional measures into one eco-friendly approach (*58*). Meanwhile, biocrusts minimize the unintended secondary damage to heritage structures such as cracking, salinization, and water accumulation that are often caused by other measures, maximally maintaining the authenticity and integrity of the structure. Furthermore, with regard to the ecological processes, biocrusts act as a natural regulator to reconfigure the hydrological cycle (*59*), heat exchange (*60*), and gas aeration (*61*) in heritage sites, shaping the microenvironmental variation of heritages sites and further providing feedback to biocrust colonization and their protective functions. Although we still do not fully understand the complex interactions among heritage deterioration factors, biocrust protective functions, and their ecological effects, it fortunately seems that biocrusts may act as a shelter and regulator to help the heritage structure endure. On this basis, we should conserve naturally occurring biocrusts on heritage structures rather than removing them and then further investigate whether biocrust colonization of heritage structures can be promoted through artificial inoculation and cultivation, which will offer a momentous nature-based intervention and research focus in the face of global climate change to preserve our shared heritage for future generations.

MATERIALS AND METHODS

Study site description

The Great Wall in this study was erected during the Chinese Ming Dynasty (1368–1644), stretching 8851.8 km in the arid and semiarid climate regions of northern China (Fig. 5) (*62*). Beyond its isolated and linear walls, the military defense system of the Great Wall encompasses a range of structures such as fortresses, barracks, beacon towers, and passes, woven into an intricate network (*1*). The construction and fortification of the Great Wall unfolded over multiple reigns in the Ming Dynasty, including Xuande, Zhengtong, Zhengde, and Jiajing emperors. The ancient Mongolian nomadic civilization, which was geographically located in northern China, posed a grave threat to the Ming Dynasty's reign. To counter these hazards, nine defense districts, including Liaodong, Jizhou, Xuandu, Datong, Shanxi, Yansui, Ningxia, Guyuan, and Gansu, were established to divide the Great Wall into different geographical regions, forming a comprehensive defense system replete with an administrative function to safeguard borders against external nomadic cavalry (*63*).

This study meticulously selected eight exemplary sections of the Great Wall as study sites, including Hengchengcun, Xingwuying, Yangjiquan, Liuyangbao, Changchengzhen, Laoyingzhen, Erfenguan, and Bianqianghao, which are geographically distributed across six counties in four provinces. The construction period of each site ranged from 1444 to 1531 and involved the structures of both fortress and wall, all belonging to the four defense districts, including Ningxia, Yansui, Shanxi, and Datong. The height above ground of sampling sites on fortresses and walls were 5.2 to 7.2 and 1.1 to 4.5 m, respectively. The studied section of the Great Wall had a similar and relatively well preservation status, which had a clearly recognizable appearance, and the extant length of walls accounted for more than 50% of the original length. The strategic selection of these study sites was based on the representation of diverse geographical and meteorological characteristics of the region where the Great Wall is located (see table S1). Specifically, these study sites encompassed both arid and semiarid climate regions, with annual precipitation, potential evaporation, wind

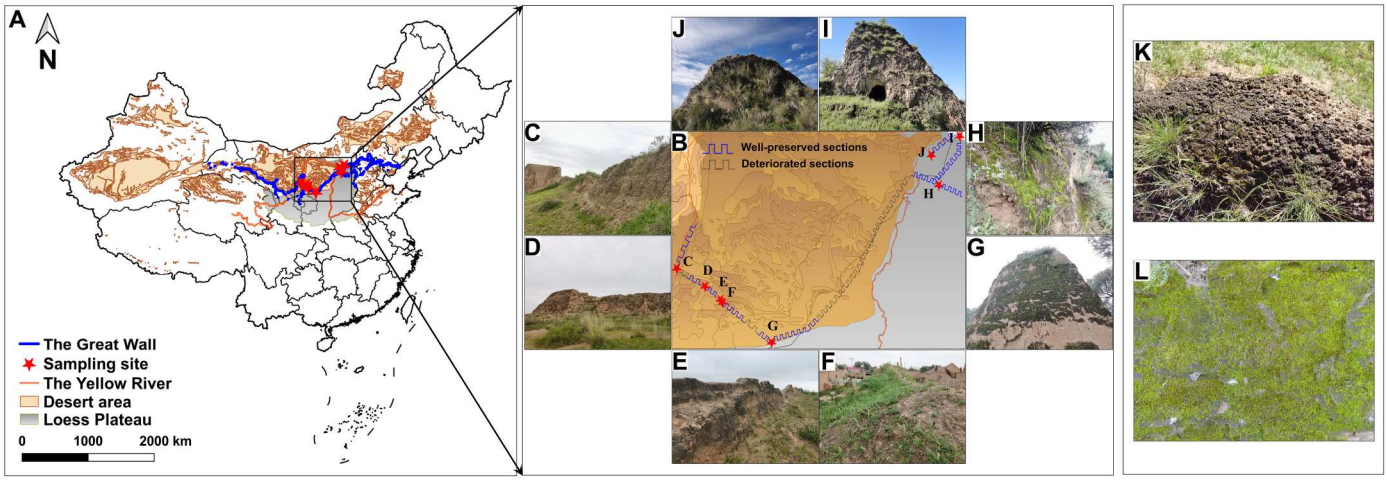

Fig. 5. Location of study sites. (**A**) Location of the Great Wall. (**B**) Zoomed in map of the sampling sites: (**C**) Hengchengcun, (**D**) Xingwuying, (**E**) Yangjiquan, (**F**) Liuyangbao, (**G**) Changchengzhen, (**H**) Laoyingzhen, (**I**) Erfenguan, and (**J**) Bianqianghao. (**K**) Cyanobacterial biocrusts. (**L**) Moss biocrusts.

speed, sunshine hours, and temperature being 192 to 483 mm, 1340 to 1750 mm, 1.3 to 2.8 m/s, 2436 to 3014 hours, and 4.2° to 8.6°C, respectively. The judicious selection of these sites ensures that the findings from this study will have broad applicability and generalizability to the larger context of the Great Wall.

Experimental design and measurements

Three experimental factors were considered in this study: biocrust types (three levels: bare rammed earth, cyanobacterial biocrusts, and moss biocrusts), climates (two levels: arid and semiarid), and structure types (two levels: wall and fortress). Overall, 12 treatments were considered, each with 10 repetitions, totaling 120 samples for the measurement of each indicator. The measurements were classified into two categories: indicators for biocrust development and parameters for biocrust functions, with the former comprising moss species, cyanobacteria genera, cover, thickness, moss density, and biomass, while the latter consisting of porosity and water-holding capacity, mechanical stability, and erodibility.

The field investigation and sampling of this study were conducted in August 2022, and the laboratory analyses were conducted from September to December 2022. Before sampling, a comprehensive investigation was conducted on the Great Wall. In each of the two climate regions, we selected two walls and two fortresses as study sites and then identified sampling plots (5.0 m by 5.0 m) with stable biocrust development and no disturbance. The spatial relationship between higher plants and biocrusts was similar in each sampling site, manifesting as sparse herbs and shrubs distributed as patches, with biocrusts embedding between them. In each of all eight study sites, five plots were selected for each biocrust type as repetitions, with the distance between the plots being 10 m, thus totaling 15 and 120 sampling plots in each study site and the entire study, respectively. Then, we measured the in situ indicators and collected one sample from every plot. According to the principles of heritage conservation, the field sampling was designed to minimize any impact on the Great Wall. Hence, the sampling was limited to the biocrust layer on the top 0 to 2 cm of rammed earth, with no damage to the actual body of the heritage structure. Meanwhile, the samples of bare rammed earth were collected from the complete chunks falling down from the main structure due to the collapse. During the sampling, the cover, thickness, penetration resistance, and shear strength were initially measured in situ using the image interpretation method (*64*), vernier caliper, WXGR-2 penetration instrument, and H-4212MH torsional shear apparatus, respectively. Consequently, biocrust samples were collected using cutting rings for subsequent laboratory analyses.

In the laboratory, the moss species were identified using optical microscope observation, and dominant cyanobacteria genera were determined by bacterial sequencing. Briefly, bacterial 16*S* ribosomal RNA gene fragments were amplified using primers 515F and 907R, and purified amplicons were sequenced on an Illumina MiSeq platform (PE250). In addition, moss density and biomass were measured by means of a sieving procedure, while soil porosity, saturated water content, and field capacity were obtained using the soil immersion method (*65*). The compressive strength was ascertained using the DDL10 biomechanical testing machine. Moreover, soil aggregate content was determined by way of the wet sieving method (*66*). As a basic component of soil structure, aggregate stability is the foundation of soil stability, further serving as an important source of soil antierodibility (*67*). Thus, three representative indicators reflecting the aggregate stability including macroaggregate content (R), GMD, and MWD were calculated through Eqs. 1 to 3 (*68*). Soil organic matter content was measured using the potassium dichromate titration method (*69*). Furthermore, the soil erodibility factor ($\boldsymbol{K}$) indicates the vulnerability of soil in response to the erosive forces, which is closely related to soil particle composition and organic matter content and is positively correlated with soil loss (*70*). The erodibility $\boldsymbol{K}$ was calculated using the Environmental policy-integrated climate (EPIC) model according to Eqs. 4 and 5 (*71*). Last, soluble salt content and electrical conductivity were obtained using the residue drying method (*72*) and SW301 conductivity meter, respectively. The fundamental physicochemical properties of biocrusts and bare rammed earth are listed in table S2. A more detailed procedure of the experiment was provided

in Supplementary Text.

$$\boldsymbol{R} = (\boldsymbol{m}_{0.25}/\boldsymbol{m}_{\mathrm{t}}) \times 100\%$$

$$\mathrm{GMD} = \mathrm{EXP}\left(\sum_{i=1}^{n} \boldsymbol{\omega}_i \ \ln \boldsymbol{X}_i\right)$$

$$\mathrm{MWD} = \sum_{i=1}^{n} \boldsymbol{X}_i \boldsymbol{\omega}_i$$

$$\boldsymbol{K} = \left\{0.2 + 0.3\mathrm{EXP}\left[-0.0256\boldsymbol{S}_{\mathrm{a}}\left(1 - \frac{\boldsymbol{S}_{\mathrm{i}}}{100}\right)\right]\right\} \times \left(\frac{\boldsymbol{S}_{\mathrm{i}}}{\boldsymbol{S}_{\mathrm{l}} - \boldsymbol{S}_{\mathrm{i}}}\right)^{0.3} \times \left[1.0 - \frac{0.25\boldsymbol{C}}{\boldsymbol{C} + \mathrm{EXP}(3.72 - 2.95\boldsymbol{C})}\right] \times \left[1.0 - \frac{0.7\boldsymbol{S}_{\mathrm{n}}}{\boldsymbol{S}_{\mathrm{n}} + \mathrm{EXP}(-5.51 + 22.9\boldsymbol{S}_{\mathrm{n}})}\right]$$

$$\boldsymbol{S}_{\mathrm{n}} = 1 - (\boldsymbol{S}_{\mathrm{a}}/100)$$

where $\boldsymbol{R}$ is the macroaggregate content (%); $\boldsymbol{m}_{0.25}$ is the weight of aggregates of >0.25 mm (in grams); $\boldsymbol{m}_{\mathrm{t}}$ is the weight of all the aggregates; GMD is the geometric mean diameter (in millimeters); $\boldsymbol{n}$ is the categories of aggregate particle size; $\boldsymbol{X}_i$ is the average diameter of the ith-order aggregate (in millimeters); $\boldsymbol{\omega}_i$ is the weight percentage of the ith-grade aggregate (%); MWD is the mean weight diameter (in millimeters); $\boldsymbol{K}$ is the erodibility coefficient; $\boldsymbol{S}_{\mathrm{a}}$ is the sand content (%); $\boldsymbol{S}_{\mathrm{i}}$ is the silt content (%); $\boldsymbol{S}_{\mathrm{l}}$ is the clay content (%); $\boldsymbol{C}$ is the organic carbon content; and $\boldsymbol{S}_{\mathrm{n}}$ is the nonsand content (%).

Data analysis

The differences in the measurements among two types of biocrusts and bare rammed earth were used to quantify biocrust characteristics and protective functions on the Great Wall. The three-way analysis of variance (ANOVA) test followed by the least significant difference test as a post hoc analysis was used to evaluate the interactions of biocrust type (cyanobacterial biocrusts, moss biocrusts, and bare rammed earth), climate (arid and semiarid), and structure type (wall and fortress) on physicochemical properties and characteristics of biocrusts at a 0.05 level of probability. The one-way ANOVA test ($\alpha = 0.05$) was used to test the differences in protective function parameters among cyanobacterial biocrusts, moss biocrusts, and bare rammed earth when other influencing factors were the same. Furthermore, the differences in protective function parameters among various defense districts were tested using one-way ANOVA ($\alpha = 0.05$), aiming to depict the macroscopic differences in the protective function of biocrusts on the regional scale. Spearman correlation analysis was used to determine the relationships between biocrust characteristics and their protective functions. The final results reflect the mean values of the repetitions, expressed as the mean value ± SE.

Supplementary Materials

This PDF file includes:
Supplementary Text
Figs. S1 to S8
Tables S1 to S5
Legends for data S1 to S8

Other Supplementary Material for this manuscript includes the following:
Data S1 to S8

REFERENCES AND NOTES

1. Y. C. Cao, Y. K. Zhang, The fractal structure of the Ming Great Wall Military Defense System: A revised horizon over the relationship between the Great Wall and the military defense settlements. *J. Cult. Herit.* **33**, 159–169 (2018).
2. R. Patalano, J. Hu, Q. Leng, W. Liu, H. Wang, P. Roberts, M. Storozum, L. Yang, H. Yang, Ancient Great Wall building materials reveal environmental changes associated with oases in northwestern China. *Sci. Rep.* **12**, 22517 (2022).
3. J. Richards, G. Zhao, H. Zhang, H. Viles, A controlled field experiment to investigate the deterioration of earthen heritage by wind and rain. *Herit. Sci.* **7**, 51 (2019).
4. L. Li, M. Shao, S. Wang, Z. Li, Preservation of earthen heritage sites on the Silk Road, northwest China from the impact of the environment. *Environ. Earth Sci.* **64**, 1625–1639 (2011).
5. J. Richards, H. Viles, Q. Guo, The importance of wind as a driver of earthen heritage deterioration in dryland environments. *Geomorphology* **369**, 107363 (2020).
6. T. Pu, W. Chen, Y. Du, W. Li, N. Su, Snowfall-related deterioration behavior of the Ming Great Wall in the eastern Qinghai-Tibet Plateau. *Nat. Hazards* **84**, 1539–1550 (2016).
7. Y. Du, W. Chen, K. Cui, K. Zhang, Study on damage assessment of earthen sites of the Ming Great Wall in Qinghai Province based on Fuzzy-AHP and AHP-TOPSIS. *Int. J. Archit. Herit.* **14**, 903–916 (2020).
8. X. Li, H. Gong, O. Zhang, W. Zhang, Y. Sun, Research on the damage of the Great Wall of Ming Dynasty in Beijing by remote sensing. *Sci. China Ser. E-Technol. Sci.* **51**, 195–202 (2008).
9. L. Reimann, A. T. Vafeidis, S. Brown, J. Hinkel, R. S. J. Tol, Mediterranean UNESCO World Heritage at risk from coastal flooding and erosion due to sea-level rise. *Nat. Commun.* **9**, 4161 (2018).
10. J. Richards, R. Bailey, J. Mayaud, H. Viles, Q. Guo, X. Wang, Deterioration risk of dryland earthen heritage sites facing future climatic uncertainty. *Sci. Rep.* **10**, 16419 (2020).
11. X. Chen, F. Bai, J. Huang, Y. Lu, Y. Wu, J. Yu, S. Bai, The organisms on rock cultural heritages: Growth and weathering. *Geoheritage* **13**, 56 (2021).
12. O. Sass, H. A. Viles, How wet are these walls? Testing a novel technique for measuring moisture in ruined walls. *J. Cult. Herit.* **7**, 257–263 (2006).
13. R. Kent, Thirlwall Castle: The use of soft capping in conserving ruined ancient monuments. *J. Archit. Conserv.* **19**, 35–48 (2013).
14. B. Weber, J. Belnap, B. Budel, A. J. Antoninka, N. N. Barger, V. B. Chaudhary, A. Darrouzet-Nardi, D. J. Eldridge, A. M. Faist, S. Ferrenberg, C. A. Havrilla, E. Huber-Sannwald, O. M. Issa, F. T. Maestre, S. C. Reed, E. Rodriguez-Caballero, C. Tucker, K. E. Young, Y. Zhang, Y. Zhao, X. Zhou, M. A. Bowker, What is a biocrust? A refined, contemporary definition for a broadening research community. *Biol. Rev.* **97**, 1768–1785 (2022).
15. E. Rodriguez-Caballero, J. Belnap, B. Büdel, P. J. Crutzen, M. O. Andreae, U. Pöschl, B. Weber, Dryland photoautotrophic soil surface communities endangered by global change. *Nat. Geosci.* **11**, 185–189 (2018).
16. J. Bethany, S. L. Johnson, F. Garcia-Pichel, High impact of bacterial predation on cyanobacteria in soil biocrusts. *Nat. Commun.* **13**, 4835 (2022).
17. T. Wang, Q. Guo, Q. Pei, W. Chen, Y. Wang, B. Zhang, J. Yu, Destruction or protection? Experimental studies on the mechanism of biological soil crusts on the surfaces of earthen sites. *Catena* **227**, 107096 (2023).
18. B. Xiao, M. A. Bowker, Y. Zhao, S. Chamizo, O. M. Issa, Biocrusts: Engineers and architects of surface soil properties, functions, and processes in dryland ecosystems. *Geoderma* **424**, 116015 (2022).
19. S. Li, M. A. Bowker, B. Xiao, Biocrust impacts on dryland soil water balance: A path toward the whole picture. *Glob. Change Biol.* **28**, 6462–6481 (2022).
20. M. L. Phillips, B. E. McNellis, A. Howell, C. M. Lauria, J. Belnap, S. C. Reed, Biocrusts mediate a new mechanism for land degradation under a changing climate. *Nat. Clim. Chang.* **12**, 71–76 (2022).
21. Q. Wang, Q. Zhang, Y. Han, D. Zhang, C.-C. Zhang, C. Hu, Carbon cycle in the microbial ecosystems of biological soil crusts. *Soil Biol. Biochem.* **171**, 108729 (2022).

22. G. Song, R. Hui, H. Yang, B. Wang, X. Li, Biocrusts mediate the plant community composition of dryland restoration ecosystems. *Sci. Total Environ.* **844**, 157135 (2022).
23. K. Jang, H. Viles, Moisture interactions between mosses and their underlying stone substrates. *Stud. Conserv.* **67**, 532–544 (2022).
24. J. Belnap, O. Lange, in *Biological Soil Crusts: Structure, Function, and Management* (Springer, 2003), pp. 182.
25. C. L. Webber, U. F. Bremer, R. Taghizadeh-Mehrjardi, B. Weber, A. Rosa, T. Scholten, S. Seitz, Biological soil crusts as a major ecosystem component in sandization areas of the Brazilian Pampa. *Geoderma Reg.* **34**, e00682 (2023).
26. A. J. Williams, B. J. Buck, D. A. Soukup, D. J. Merkler, Geomorphic controls on biological soil crust distribution: A conceptual model from the Mojave Desert (USA). *Geomorphology* **195**, 99–109 (2013).
27. M. T. Lehtonen, Y. Takikawa, G. Ronnholm, M. Akita, N. Kalkkinen, E. Ahola-Iivarinen, P. Somervuo, M. Varjosalo, J. P. T. Valkonen, Protein secretome of moss plants (physcomitrella patens) with emphasis on changes induced by a fungal elicitor. *J. Proteome Res.* **13**, 447–459 (2014).
28. E. Couradeau, V. Felde, D. Parkinson, D. Uteau, A. Rochet, C. Cuellar, G. Winegar, S. Peth, T. R. Northen, F. Garcia-Pichel, *In situ* x-ray tomography imaging of soil water and cyanobacteria from biological soil crusts undergoing desiccation. *Front. Environ. Sci.* **6**, 65 (2018).
29. G. Mugnai, F. Rossi, V. Felde, C. Colesie, B. Budel, S. Peth, A. Kaplan, R. De Philippis, The potential of the cyanobacterium *Leptolyngbya ohadii* as inoculum for stabilizing bare sandy substrates. *Soil Biol. Biochem.* **127**, 318–328 (2018).
30. P. Varuni, S. N. Menon, G. I. Menon, Phototaxis as a collective phenomenon in cyanobacterial colonies. *Sci. Rep.* **7**, 17799 (2017).
31. A. Sepehr, M. Hassanzadeh, E. Rodriguez-Caballero, The protective role of cyanobacteria on soil stability in two Aridisols in northeastern Iran. *Geoderma Reg.* **16**, 201 (2019).
32. J. Kou, C. Feng, X.-L. Bai, H. Chen, Morphology and taxonomy of leaf papillae and mammillae in Pottiaceae of China. *J. Syst. Evol.* **52**, 521–532 (2014).
33. M. C. F. Proctor, The bryophyte paradox: Tolerance of desiccation, evasion of drought. *Plant Ecol.* **151**, 41–49 (2000).
34. B. Xiao, F. H. Sun, K. L. Hu, G. J. Kidron, Biocrusts reduce surface soil infiltrability and impede soil water infiltration under tension and ponding conditions in dryland ecosystem. *J. Hydrol.* **568**, 792–802 (2019).
35. G. J. Kidron, Y. Wang, M. Herzberg, Exopolysaccharides may increase biocrust rigidity and induce runoff generation. *J. Hydrol.* **588**, 125081 (2020).
36. J. Yue, X. Huang, L. Zhao, Z. Wang, Study on the factors affecting cracking of earthen soil under dry shrinkage and freeze-thaw conditions. *Sci. Rep.* **12**, 1816 (2022).
37. S. Peng, T. Guo, G. Liu, The effects of arbuscular mycorrhizal hyphal networks on soil aggregations of purple soil in southwest China. *Soil Biol. Biochem.* **57**, 411–417 (2013).
38. B. Cania, G. Vestergaard, M. Suhadolc, R. Mihelǐ, M. Krauss, A. Fliessbach, P. Mäder, A. Szumelda, M. Schloter, S. Schulz, Site-specific conditions change the response of bacterial producers of soil structure-stabilizing agents such as exopolysaccharides and lipopolysaccharides to tillage intensity. *Front. Microbiol.* **11**, 568 (2020).
39. W. Yang, Z. Li, C. Cai, Z. Guo, J. Chen, J. Wang, Mechanical properties and soil stability affected by fertilizer treatments for an Ultisol in subtropical China. *Plant and Soil* **363**, 157–174 (2013).
40. B. Chang, H. Wen, C. W. Yu, X. Luo, Z. Gu, Preservation of earthen relic sites against salt damages by using a sand layer. *Indoor Built Environ.* **31**, 1142–1156 (2022).
41. Y. Zhang, W. Ye, Y. Chen, B. Chen, Impact of NaCl on drying shrinkage behavior of low-plasticity soil in earthen heritages. *Can. Geotech. J.* **54**, 1762–1774 (2017).
42. S. M. F. Rabbi, B. Minasny, A. B. McBratney, L. M. Young, Microbial processing of organic matter drives stability and pore geometry of soil aggregates. *Geoderma* **360**, 114033 (2020).
43. B. Xiao, M. A. Bowker, Moss-biocrusts strongly decrease soil surface albedo, altering land-surface energy balance in a dryland ecosystem. *Sci. Total Environ.* **741**, 140425 (2020).
44. H. A. Viles, N. A. Cutler, Global environmental change and the biology of heritage structures. *Glob. Change Biol.* **18**, 2406–2418 (2012).
45. X. Liu, Y. Qian, F. Wu, Y. Wang, W. Wang, J.-D. Gu, Biofilms on stone monuments: Biodeterioration or bioprotection? *Trends Microbiol.* **30**, 816–819 (2022).
46. G. Zhang, C. Gong, J. Gu, Y. Katayama, T. Someya, J.-D. Gu, Biochemical reactions and mechanisms involved in the biodeterioration of stone world cultural heritage under the tropical climate conditions. *Int. Biodeterior. Biodegrad.* **143**, 104723 (2019).
47. N. A. Cutler, H. A. Viles, S. Ahmad, S. McCabe, B. J. Smith, Algal 'greening' and the conservation of stone heritage structures. *Sci. Total Environ.* **442**, 152–164 (2013).
48. N. Cutler, H. Viles, Eukaryotic microorganisms and stone biodeterioration. *Geomicrobiol. J.* **27**, 630–646 (2010).
49. S. Kammann, U. Schiefelbein, C. Dolnik, T. Mikhailyuk, E. Demchenko, U. Karsten, K. Glaser, Successional development of the phototrophic community in biological soil crusts on coastal and inland dunes. *Biology-Basel* **12**, 58 (2023).
50. D. J. Eldridge, M. Delgado-Baquerizo, The influence of climatic legacies on the distribution of dryland biocrust communities. *Glob. Change Biol.* **25**, 327–336 (2019).
51. Y. Han, Q. Wang, Q. Li, C. Hu, Active metabolism and biomass dynamics of biocrusts are shaped by variation in their successional state and seasonal energy sources. *Sci. Total Environ.* **831**, 154756 (2022).
52. Y. K. Zhang, S. Y. Li, L. F. Tan, J. Y. Zhou, Distribution and integration of military settlements' cultural heritage in the large pass city of the Great Wall in the Ming Dynasty: A case study of Juyong Pass defense area. *Sustainability* **13**, 7166 (2021).
53. T. Cudahy, P. Shi, Y. Novikova, B. Fu, Satellite ASTER mineral mapping the provenance of the loess used by the Ming to build their earthen Great Wall. *Remote Sens. (Basel)* **12**, 270 (2020).
54. W. Liu, X. Zhou, T. Jin, Y. Li, B. Wu, D. Yu, Z. Yu, B. Su, R. Chen, Y. Feng, M. Delgado-Baquerizo, Multikingdom interactions govern the microbiome in subterranean cultural heritage sites. *Proc. Natl. Acad. Sci. U.S.A.* **119**, e2121141119 (2022).
55. S. V. Hanssen, H. A. Viles, Can plants keep ruins dry? A quantitative assessment of the effect of soft capping on rainwater flows over ruined walls. *Ecol. Eng.* **71**, 173–179 (2014).
56. A. Arizzi, H. Viles, G. Cultrone, Experimental testing of the durability of lime-based mortars used for rendering historic buildings. *Construct. Build Mater.* **28**, 807–818 (2012).
57. D. Qiu, M. A. Bowker, B. Xiao, Y. Zhao, X. Zhou, X. Li, Mapping biocrust distribution in China's drylands under changing climate. *Sci. Total Environ.* **905**, 167211 (2023).
58. M. Shan, Y.-F. Chen, Z. Zhai, J. Du, Investigating the critical issues in the conservation of heritage building: The case of China. *J. Build. Eng.* **51**, 104319 (2022).
59. S. L. Li, M. A. Bowker, B. Xiao, Impacts of moss-dominated biocrusts on rainwater infiltration, vertical water flow, and surface soil evaporation in drylands. *J. Hydrol.* **612**, 128176 (2022).
60. S. Li, F. Sun, S. Chamizo, B. Xiao, Towards moss-dominated biocrust effects on soil temperature across seasons in drylands: Insight from continuous measurements of soil thermal properties and solar radiation. *Geoderma* **421**, 115911 (2022).
61. F. Sun, B. Xiao, G. J. Kidron, J. L. Heitman, Insights about biocrust effects on soil gas transport and aeration in drylands: Permeability, diffusivity, and their connection to hydraulic conductivity. *Geoderma* **427**, 116137 (2022).
62. M. M. Su, G. Wall, Community participation in tourism at a world heritage site: Mutianyu Great Wall, Beijing, China. *Int. J. Tour. Res.* **16**, 146–156 (2014).
63. Y. Du, W. Chen, K. Cui, Z. Guo, G. Wu, X. Ren, An exploration of the military defense system of the Ming Great Wall in Qinghai province from the perspective of castle-based military settlements. *Archaeol. Anthropol. Sci.* **13**, 46 (2021).
64. M. A. Bowker, N. C. Johnson, J. Belnap, G. W. Koch, Short-term monitoring of aridland lichen cover and biomass using photography and fatty acids. *J. Arid Environ.* **72**, 869–878 (2008).
65. J. Mao, Y. Li, J. Zhang, K. Zhang, X. Ma, G. Wang, L. Fan, Organic carbon and silt determining subcritical water repellency and field capacity of soils in arid and semi-arid region. *Front. Environ. Sci.* **10**, 1031237 (2022).
66. S. Han, M. Delgado-Baquerizo, X. Luo, Y. Liu, J. D. Van Nostrand, W. Chen, J. Zhou, Q. Huang, Soil aggregate size-dependent relationships between microbial functional diversity and multifunctionality. *Soil Biol. Biochem.* **154**, 108143 (2021).
67. L. de la Torre-Robles, C. Muñoz-Robles, E. Huber-Sannwald, J. A. Reyes-Agüero, Functional stability: From soil aggregates to landscape scale in a region severely affected by gully erosion in semi-arid central Mexico. *Catena* **222**, 106864 (2023).
68. R. Ma, F. Hu, C. Xu, J. Liu, S. Zhao, Response of soil aggregate stability and splash erosion to different breakdown mechanisms along natural vegetation restoration. *Catena* **208**, 105775 (2022).
69. D. K. Benbi, Evaluation of a rapid microwave digestion method for determination of total organic carbon in soil. *Commun. Soil Sci. Plant Anal.* **49**, 2103–2112 (2018).
70. R. Raj, M. Saharia, S. Chakma, Mapping soil erodibility over India. *Catena* **230**, 107271 (2023).
71. L. Gao, M. A. Bowker, M. Xu, H. Sun, D. Tuo, Y. Zhao, Biological soil crusts decrease erodibility by modifying inherent soil properties on the Loess Plateau, China. *Soil Biol. Biochem.* **105**, 49–58 (2017).
72. K. Akhtar, W. Wang, G. Ren, A. Khan, Y. Feng, G. Yang, Changes in soil enzymes, soil properties, and maize crop productivity under wheat straw mulching in Guanzhong, China. *Soil Tillage Res.* **182**, 94–102 (2018).

Acknowledgments: We express thanks to S. Shen for assistance in the field investigation and sampling. **Funding:** This work was supported by the National Natural Science Foundation of China (no. 42077010) and the "Light of West China" Program of the Chinese Academy of Sciences (no. 2019). **Author contributions:** Conceptualization: B.X. Data curation: B.X. Formal analysis: B.X. Funding acquisition: B.X. Investigation: B.X. and Y.C. Methodology: B.X. and Y.C. Project administration: B.X. Resources: B.X. Supervision: B.X. Validation: B.X. Visualization: B.X. and Y.C. Writing—original draft: B.X. and Y.C. Writing—review and editing: B.X., Y.C., M.D.-B., and

M.A.B. **Competing interests:** The authors declare that they have no competing interests. **Data and materials availability:** All data needed to evaluate the conclusions in the paper are present in the paper and/or the Supplementary Materials. The data for this study have been simultaneously deposited in the database Dryad: https://doi.org/10.5061/dryad.xd2547dpr.

Submitted 30 August 2023
Accepted 9 November 2023
Published 8 December 2023
10.1126/sciadv.adk5892